A PPy/ZnO functional interlayer to enhance electrochemical performance of lithium/ sulfur batteries

Fuxing Yin[1], Jun Ren[1], Yongguang Zhang[1*], Taizhe Tan[2] and Zhihong Chen[3*]

Abstract

To enhance the electrochemical performance of the lithium/sulfur batteries, a novel interlayer was prepared by coating the slurry of PPy/ZnO composite onto the surface of a separator. Owing to a three-dimensional hierarchical network structure, PPy/ZnO composite serves as a polysulfide diffusion absorbent that can intercept the migrating soluble polysulfides to enhance the electrochemical performance of the Li/S batteries. The specific capacity of the cell with PPy/ZnO interlayer remained at 579 mAh g^{-1} after 100 cycles at 0.2 C. This interlayer can provide novel avenues for the commercial applications of Li/S batteries.

Keywords: Lithium/sulfur battery, PPy/ZnO composite, Interlayer, Electrochemical performance

Background

With the increasing development of the portable electronic devices and negative impact of conventional energy systems, the development of high-performing, lightweight energy storage systems has attracted significant attention. Lithium/sulfur (Li/S) batteries are regarded as a likely alternative because of their high energy density of 2600 Wh kg^{-1} and theoretical capacity of 1672 mAh g^{-1} [1, 2]. However, their performance is limited by low-conductivity of active material and the polysulfide shuttle mechanism [3–5].

In the last few decades, several strategies have been tested to overcome these challenges, such as encapsulation of the active material within nanostructure, development of novel electrolytes, and binder modification [6–9]. The insertion of an interlayer between cathode and separator can significantly improve the capacity retention by trapping polysulfides [10–12]. However, a low adsorption capacity of carbon for polysulfides still restricts the cycling performance of Li/S batteries. Studies demonstrate that PPy is a proton-doped type of conductive polymer. This type of conductive polymer can adsorb polysulfides by H bonds. Therefore, PPy is suitable for fabrication as an interlayer to suppress the shuttling of polysulfides [13]. Also, the polar metal oxides can form chemical bonds with polysulfides to decrease the loss of active materials [14–16]. Yu et al. [17] have reported that ZnO coating could effectively confine polysulfides during cycling. However, these metal oxides reduce the utilization of sulfur due to their low electrical conductivity.

After comprehensive considerations, in order to realize the high performance of Li/S batteries, a novel interlayer composed of polypyrrole (PPy) and ZnO nanoparticle has been fabricated. The cross-linked PPy nanofibers formed a three-dimensional hierarchical network structure in the composite which was uniformly coated by ZnO nanoparticles. We hypothesized that the interlayer with special morphology would provide both the chemical and physical restraints to hinder the diffusion of polysulfides and protect the active material to suppress "shuttle effect." The combination of PPy and ZnO not only enhances the ability of the interlayer to capture polysulfide but also avoids the defect of poor conductivity of the ZnO-only interlayer. Moreover, such a 3D structure can offer better electronic pathways and reduce the electrochemical polarization. To prove the effectiveness of such an interlayer in

* Correspondence: yongguangzhang@hebut.edu.cn; chenzhihong1227@sina.com
[1]School of Materials Science and Engineering, Research Institute for Energy Equipment Materials, Hebei University of Technology, Tianjin 300130, China
[3]Shenyang Institute of Automation, Chinese Academy of Sciences, Guangzhou 511458, China
Full list of author information is available at the end of the article

Yin *et al. Nanoscale Research Letters* (2018) 13:307

Page 2 of 7

enhancing the performance of Li/S batteries, we uniformly coated PPy/ZnO composite onto the surface of a separator as an interlayer.

Methods

Preparation of PPy/ZnO interlayer

PPy nanofiber network was synthesized as previously reported [18]. The as-prepared PPy (0.2 g) was added in Zn $(CH_3COO)_2 \cdot 2H_2O$ methanol solution (4 mM, 30 mL) under magnetic stirring. Then, potassium hydroxide (KOH) methanol solution (0.3 M, 10 mL) was added and the mixture was transferred into an oil bath at 60 C under continuous stirring. Finally, the PPy/ZnO composite was obtained by centrifugation. The mixed slurry of PPy/ZnO composite, Ketjen Black (EC 300 J), and polyvinylidene fluoride (PVDF) (80:10:10 in weight ratio) was coated uniformly onto the surface of the separator (Celgard 2300) to fabricate interlayer.

Preparation of S-cathode

Sulfur (Sigma-Aldrich, ~ 100 mesh particle size) and graphene were thoroughly mixed in the weight ratio of 2:1 and then heated at 155 C for 12 h under argon atmosphere. The sulfur cathode was fabricated by mixing S/graphene composite, Ketjen Black, and PVDF (80:10:10 in weight ratio). The slurry was smeared on carbon-coated aluminum foil. After drying at 60 C for 12 h, the cathode was obtained by punching using a disk with 14 nm-in-diameter. The sulfur loading is approximately 1.3 mg cm^{-2}.

Material characterization

The samples were characterized by field emission scanning electron microscopy (FE-SEM, Leo-1530), transmission electron microscopy (TEM, JEM-2100F), X-ray diffractometer (XRD, Smart Lab), Fourier-transform infrared spectroscopy (FTIR, TENSOR 27), and X-ray photoelectron spectroscopy (XPS, Thermo ESCALAB 250Xi).

Electrochemical measurements

The half-cell assembly was developed in a glove-box filled with Ar (99.9995% purity). Lithium foil was applied as the anode and a mixed solution of 1 M LiN $(CF_3SO_2)_2$ (LiTFSI) with 0.1 M LiNO$_3$ dissolved in a solution of 1,3-dioxolane (DOL) and 1,2-dimethoxyethane (DME) (*v/v* 10:10) was prepared as electrolyte. The amount of electrolyte is around 30 μL. The as-made half-cell was tested in the voltage range of 1.7–2.8 V using battery testing station (Neware). The VersaSTAT 4 electrochemical workstation was performed to test cyclic voltammetry (CV, 1.7–2.8 V) and electrochemical impedance spectroscopy (EIS, 10^{-2}–10^5 Hz). The scan rate of CV was 0.1 mV s^{-1}.

Results and discussion

The structure of the cell with PPy/ZnO interlayer is shown in Fig. 1. The PPy/ZnO composite was coated uniformly onto the surface of the separator to fabricate interlayer to trap polysulfides.

SEM and TEM were employed to investigate the morphology and size of PPy/ZnO composite. As seen in Fig. 2a, PPy/ZnO composite was obtained with a three-dimensional hierarchical network structure made up of cross-linked nanofibers. The ZnO nanoparticles were clearly present in the composite (Fig. 2c) and grew uniformly on the surface of PPy nanofiber (Fig. 2b). The diameter of PPy nanofiber and ZnO nanoparticle was about ~ 80 nm and ~ 15 nm, respectively. Clear lattice fringes can be observed in Fig. 2c indicating the presence of ZnO with the various lattice spacing of 0.24 and 0.28 nm, which can be assigned to (101) plane and (100) plane, respectively. The thickness of PPy/ZnO interlayer was estimated to be around 12.4 nm from the cross-sectional images via SEM (Fig. 2d).

Figure 3a displays the XRD patterns of PPy and PPy/ZnO composite. We can observe a diffraction peak at about 24°, a characteristic of PPy, which corresponds to a typical amorphous character [19]. The PPy/ZnO composite presented the typical diffraction peaks of the hexagonal wurtzite structure of ZnO (JCPDS card No. 36-1451). FTIR spectra of PPy and PPy/ZnO composite recorded in the range of 400–2000 cm^{-1} are presented in Fig. 3b. The characteristic bands of PPy at 1533 and 1456 cm^{-1} were attributed to the pyrrole ring fundamental vibrations. The bands at around 1033, 1164, and 1286 cm^{-1} were assigned to N-H, C-N-C, and = C-H, respectively [20]. In the spectrum of PPy/ZnO composite, the peak at 437 cm^{-1} was attributed to Zn-O stretching vibration of ZnO.

The electrochemical performance of the as-prepared cell with PPy/ZnO interlayer and without PPy/ZnO
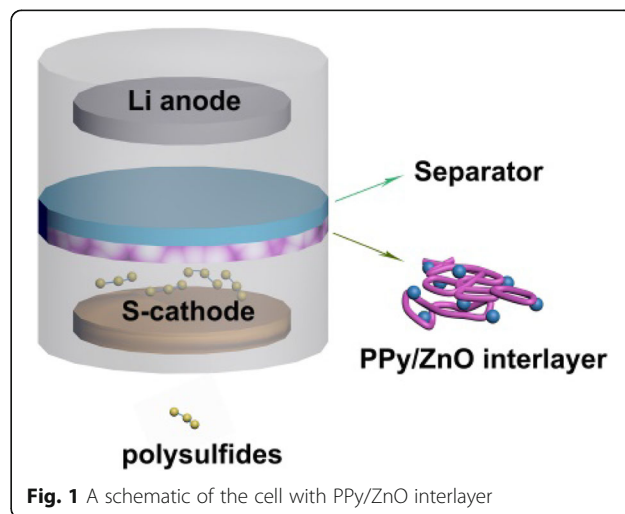

Fig. 1 A schematic of the cell with PPy/ZnO interlayer

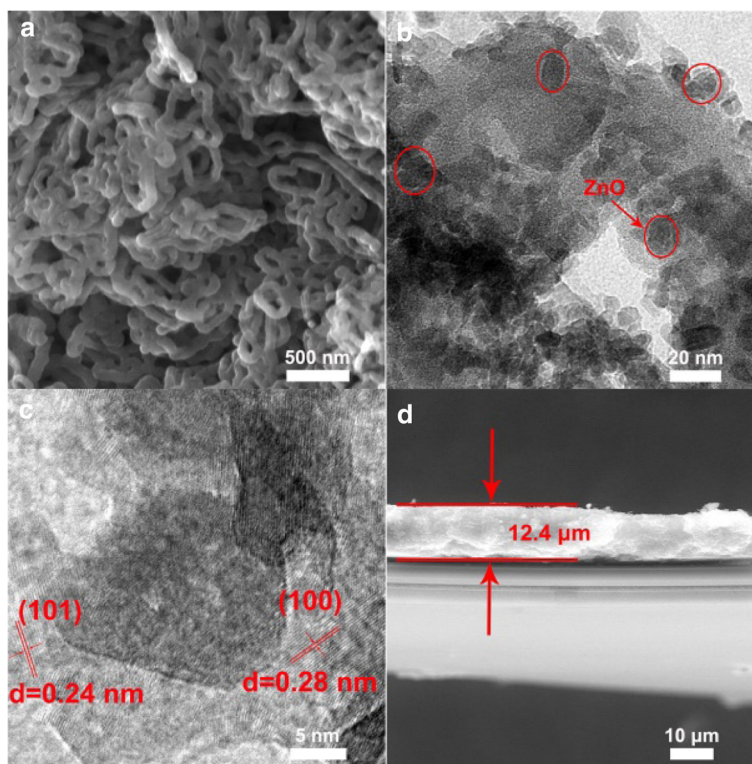Yin *et al. Nanoscale Research Letters* (2018) 13:307

Page 3 of 7

Fig. 2 a SEM image of PPy/ZnO composite. **b–c** TEM images of PPy/ZnO composite at different magnifications. **d** cross-sectional SEM image of PPy/ZnO composite-coated separator

interlayer is shown in Fig. 4. All the CV curves show two reduction peaks and two oxidation peaks. Two reduction peaks are related to the active material forming higher order polysulfides (Li_2S_n, $4 \leq n \leq 8$) and a further reduction to form lower order polysulfides (Li_2S_2/Li_2S), respectively [21–23]. Two oxidation peaks correspond to the conversion of Li_2S_2/Li_2S into higher order polysulfides further to S [24]. By comparing the peak positions, the insertion of PPy/ZnO interlayer can reduce the

kinetic barrier for the redox reaction of active material and possibly lower the electrochemical polarization [25].

Galvanostatic charge/discharge voltage profiles were measured at 0.2 C to investigate the cycle performances of the as-prepared Li/S batteries. Fig. 5a, b present the charge/discharge profiles in the 1st, 5th, 10th, 50th, and 100th cycles. These profiles are in good agreement with the CV measurements. Compared with the cell without PPy/ZnO interlayer, the cell with PPy/
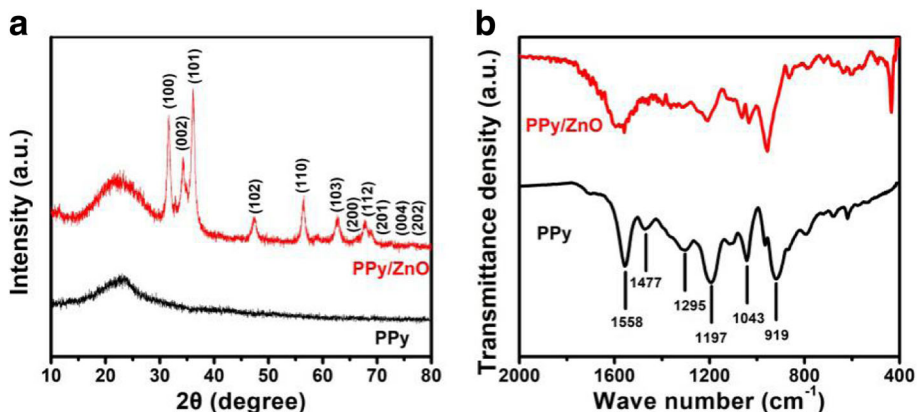

Fig. 3 a XRD patterns of the PPy and PPy/ZnO composite and **b** FTIR spectra of PPy and PPy/ZnO composite
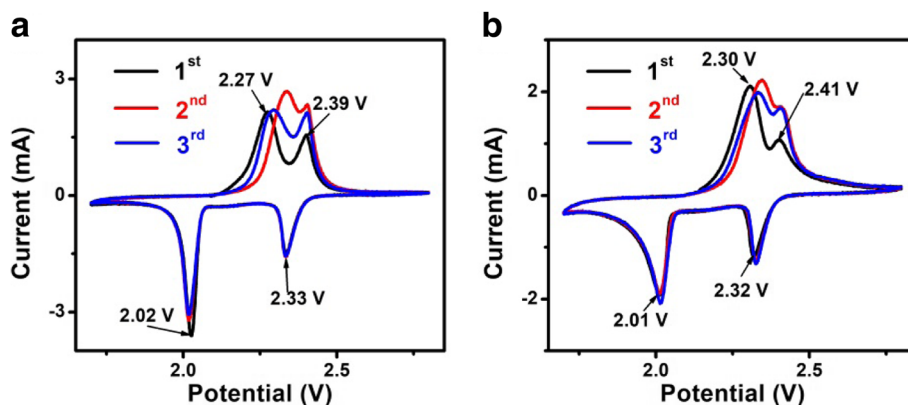
Yin *et al. Nanoscale Research Letters* (2018) 13:307

Page 4 of 7

Fig. 4 CV profiles of cells with PPy/ZnO interlayer (**a**) and without PPy/ZnO interlayer (**b**)

ZnO interlayer has lower difference between the long lower discharge plateau and charge plateau. In other words, the cell with PPy/ZnO interlayer had a lower ΔE value than the one without PPy/ZnO interlayer. These results are consistent with the CV curves peaks and further indicate that PPy/ZnO interlayer can reduce the polarization. Also, the cell with PPy/ZnO interlayer revealed more stable discharge plateaus than that without PPy/ZnO interlayer.

The cell with PPy/ZnO interlayer exhibited an initial capacity of 1194 mAh g^{-1} and still delivered a discharge capacity of 579 mAh g^{-1} at 0.2 C after 100 cycles (Fig. 5c). In contrast, the capacity of Li/S batteries without PPy/ZnO interlayer was reduced to 318 mAh g^{-1} after 100 cycles, revealing serious capacity fading (Additional file 1). Hence, by inserting the interlayer, the initial discharge capacity is significantly increased and the capacity decay rate is
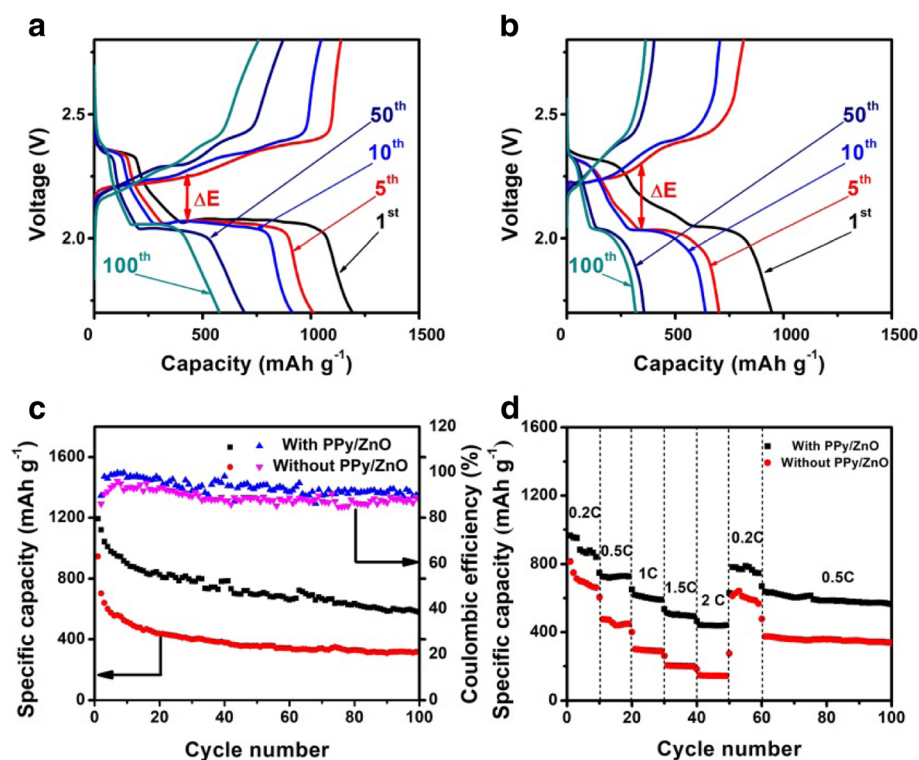

Fig. 5 Galvanostatic charge/discharge profiles of cells with PPy/ZnO interlayer (**a**), without PPy/ZnO interlayer (**b**) at 0.2 C; the cycling performance at 0.2 C (**c**) and rate performance (**d**) of cells with PPy/ZnO interlayer and without PPy/ZnO interlayer

Yin *et al. Nanoscale Research Letters* (2018) 13:307

Page 5 of 7

significantly reduced. These results further illustrate that the polysulfides are absorbed by PPy/ZnO interlayer instead of diffusing to the anode and the interlayer can remarkably promote the reuse of active materials [26].

The as-prepared Li/S batteries with or without PPy/ZnO interlayer were also tested at varying current densities between 0.2 C and 2 C. The discharge capacities of the cell with PPy/ZnO interlayer were approximately 951, 718, 609, 501, and 404 mAh g^{-1} at 0.2 C, 0.5 C, 1 C, 1.5 C, and 2 C, respectively (Fig. 5d). A stable capacity of 770 mAh g^{-1} resumed when the current rate was returned back to 0.2 C. The cell without PPy/ZnO interlayer delivered 714 mAh g^{-1}, 472 mAh g^{-1}, 295 mAh g^{-1}, 202 mAh g^{-1}, and 144 mAh g^{-1} at 0.2 C, 0.5 C, 1 C, 1.5 C, and 2 C, respectively. When the current rate was switched back to 0.5 C, the reversible capacity (564 mAh g^{-1}) of the cell with PPy/ZnO interlayer after 40 cycles was higher than that without PPy/ZnO interlayer. These results further validate the excellent cycling stability of the cell with PPy/ZnO interlayer. The possible reason for the phenomenon could be that PPy/ZnO composite as functional interlayer with ultrahigh adsorption capability can limit the dissolution and diffusion of polysulfides to enhance cycling stability [23].

We performed EIS measurements to further investigate the effect of the PPy/ZnO interlayer on charge transfer (Fig. 6). In the high-frequency region, the intercept on the real axis and a depressed semicircle are ascribed to electrolyte ohmic resistance (R_o) and the charge transfer resistance (R_{ct}), respectively. The tilted straight line in the low-frequency region is ascribed to Warburg impedance [27]. As shown in Fig. 6a, the R_{ct} was reduced from 66.3 Ω to 35.9 Ω after the insertion of PPy/ZnO interlayer, which could be because the three-dimensional network of PPy/ZnO interlayer provides faster charge transfer [28]. Even after 50 cycles, the R_{ct} for the cell with PPy/ZnO interlayer (12 Ω) was much smaller than that without PPy/ZnO interlayer (33.4 Ω). These results suggest that the PPy/ZnO interlayer not only increases the utilization of active

materials but also accelerates fast charge collection/transport [29]. Meanwhile, the difference of Warburg impedance in Fig. 6 was attributed to the fact that the ZnO nanoparticles act positively rather than hinder the diffusion of ions [30].

To further investigate the role of PPy/ZnO interlayer in capturing the polysulfides in Li/S batteries, the cell was dismantled after cycling and the bonding configurations of the PPy/ZnO interlayer were studied using C 1 s, N 1 s, S 2p, and Zn 2p XPS spectra (Fig. 7). The samples revealed a strong peak of C-C at about 248.7 eV and multiple peaks between 285 and 292 eV. These multiple peaks correspond to bonds between the hetero atoms or oxygen and carbon, showing the presence of C-N/C-S, C-O, C=O, and O-C=O bonds. As shown in Fig. 7b, there were strong multiple peaks in the range of 398 and 402 eV, namely at 398.9, 399.8, and 400.6 eV, which were ascribed to pyridinic-N, pyrrolic-N, and graphitic-N, respectively. The presence of nitrogen functional groups facilitates the adsorption of the active material during cycling. The sulfur peaks were concentrated in the range of 166 to 172 eV (Fig. 7c). The peak located at 167.2 eV was ascribed to thiosulfate, which is formed due to polysulfide oxidation on the ZnO surface. The other two peaks at around 169.3 to 170.5 eV were attributed to the presence of electrolyte [31]. These results further proved that ZnO nanoparticles can improve the absorption and retention of polysulfides. As presented in the high-resolution Zn 2p XPS spectrum (Fig. 7d), the two peaks centered at 1022.3 and 1045.1 eV are similar to the reported peaks of Zn 2p3/2 and ZnO 2p1/2 [32]. Hence, PPy/ZnO interlayer can absorb and limit polysulfides owing to the strong interaction between PPy/ZnO and polysulfides, which can effectively relax the shuttle effect in Li/S batteries.

Conclusions

A unique interlayer consisting of a three-dimensional hierarchical network PPy uniformly covered with ZnO nanoparticles was successfully prepared. The prepared interlayer can minimize polysulfide shuttling and
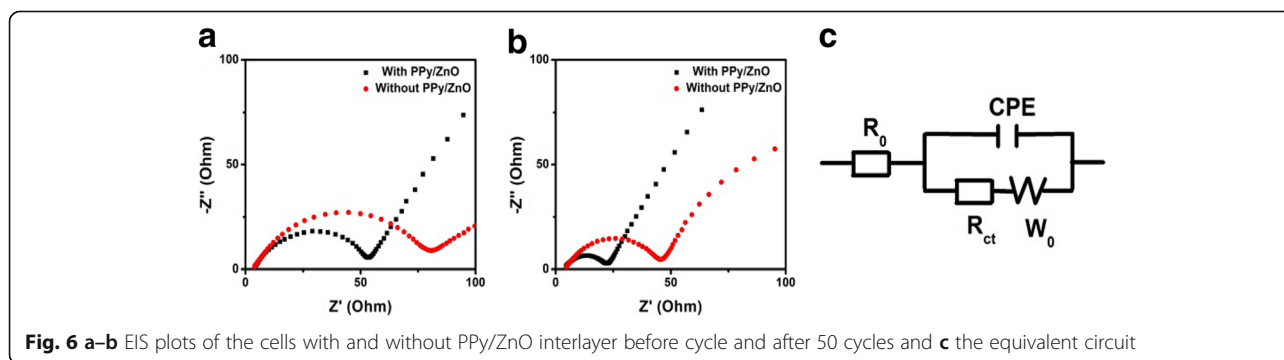
Fig. 6 a–b EIS plots of the cells with and without PPy/ZnO interlayer before cycle and after 50 cycles and **c** the equivalent circuit
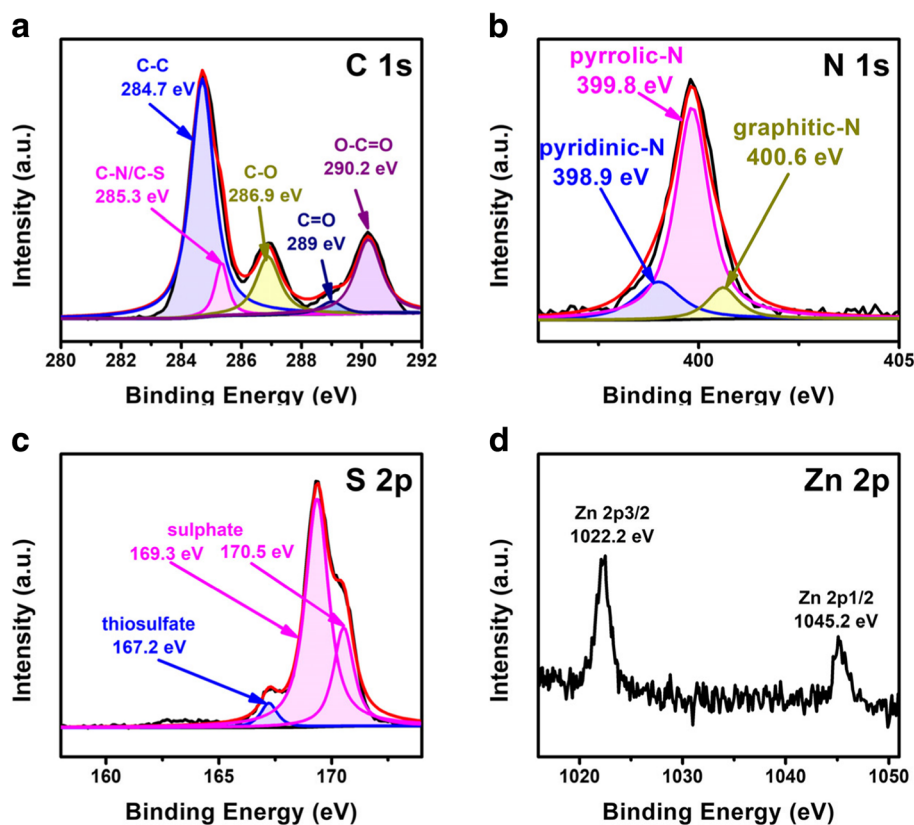
Yin et al. Nanoscale Research Letters (2018) 13:307

Page 6 of 7

Fig. 7 XPS spectra of C 1 s (**a**), N 1 s (**b**), S 2p (**c**), and Zn2p (**d**)

effectively protect Li anode to prolong cycle life and improve rate performance of Li/S batteries. The improved performance can be attributed to the physical and chemical interactions of unique three-dimensional hierarchical network structure, nitrogen functional groups, and ZnO nanoparticles to reutilize the dissolved polysulfides. Hence, these preliminary results demonstrate that PPy/ZnO interlayer is a promising strategy for the development of actual applications of high-performance Li/S batteries.

Additional file

Additional file 1: Figure S1. The cycling performance at 0.2 C of cells with PPy/ZnO interlayer, with PPy and without interlayer. (DOC 695 kb)

Abbreviations
CV: Cyclic voltammetry; DME: 1,2-Dimethoxyethane; DOL: 1,3-Dioxolane; EIS: Electrochemical impedance spectroscopy; FTIR: Fourier-transform infrared spectroscopy; KOH : Potassium hydroxide; Li/S: Lithium/sulfur; LiTFSI: Lithium bis(trifluoromethanesulfonyl)imide; PPy: Polypyrrole; PVDF: Polyvinylidene fluoride; SEM: Scanning electron microscope; TEM: Transmission electron microscope; XPS: X-ray photoelectron spectroscopy; XRD: X-ray diffraction; ZnO: Zinc oxide

Availability of data and materials
All data generated or analyzed during this study are included in this published article.

Authors' contributions
YZ conceived and designed the experiments. FY and JR carried out the experiments. FY, JR, and TT analyzed the data. TT, FY, and ZC contributed in the drafting and revision of the manuscript. YZ and ZC supervised the work and finalized the manuscript. All authors read and approved the final manuscript.

Competing interests
The authors declare that they have no competing interests.

Publisher's Note
Springer Nature remains neutral with regard to jurisdictional claims in published maps and institutional affiliations.

Author details
[1]School of Materials Science and Engineering, Research Institute for Energy Equipment Materials, Hebei University of Technology, Tianjin 300130, China. [2]Synergy Innovation Institute of GDUT, Heyuan, Guangdong Province, China. [3]Shenyang Institute of Automation, Chinese Academy of Sciences, Guangzhou 511458, China.

References

1. Wang DW, Zeng Q, Zhou G, Yin L, Li F, Cheng HM, Gentle IR, Lu GQM (2013) Carbon–sulfur composites for Li–S batteries: status and prospects. J Mater Chem A 1:9382–9394
2. Lin Z, Liang C (2014) Lithium-sulfur batteries: from liquid to solid cells. J Mater Chem A 3:936–958
3. Liu J, Qian T, Wang M, Liu X, Xu N, You Y, Yan C (2017) Molecularly imprinted polymer enables high-efficiency recognition and trapping lithium polysulfides for stable lithium sulfur battery. Nano Lett 17:5064–5070
4. Lei TY, Chen W, Huang JW, Yan CY, Sun HX, Wang C, Zhang WL, Li YR, Xiong J (2016) Multi-functional layered WS_2 nanosheets for enhancing the performance of lithium-sulfur batteries. Adv Energy Mater 7:1601843–1601850
5. Lei TY, Xie YM, Wang XF, Miao SY, Xiong J, Yan CL (2017) TiO_2 feather duster as effective polysulfides restrictor for enhanced electrochemical kinetics in lithium-sulfur batteries. Small 13:1701013–1701021
6. Yu XW, Manthiram A (2017) Electrode-electrolyte interfaces in lithium-sulfur batteries with liquid or inorganic solid electrolytes. Acc Chem Res 50:2653–2660
7. Chen W, Lei TY, Wu CY, Deng M, Gong CH, Hu K, Ma YC, Dai LP, Lv WQ, He WD (2018) Designing safe electrolyte systems for a high-stability lithium-sulfur battery. Adv Energy Mater 8:1702348–1702371
8. Chen W, Qian T, Xiong J, Xu N, Liu X, Liu J, Zhou J, Shen X, Yang T, Chen Y (2017) A new type of multifunctional polar binder: toward practical application of high energy lithium sulfur batteries. Adv Mater 29:1605160–1605166
9. Chen W, Lei TY, Qian T, Lv WQ, He WD, Wu CY, Liu XJ, Liu J, Chen B, Yan CL, Xiong J (2018) A new hydrophilic binder enabling strongly anchoring polysulfides for high-performance sulfur electrodes in lithium-sulfur battery. Adv Energy Mater 8:1702348–1702355
10. Sun J, Sun Y, Pasta M, Zhou G, Li Y, Liu W, Xiong F, Cui Y (2016) Entrapment of polysulfides by a black-phosphorus-modified separator for lithium-sulfur batteries. Adv Mater 28:9797–9803
11. Su YS, Manthiram A (2012) Lithium-sulphur batteries with a microporous carbon paper as a bifunctional interlayer. Nat Commun 3:1166–1172
12. Liu M, Li Q, Qin X, Liang G, Han W, Zhou D, He YB, Li B, Kang F (2017) Suppressing self-discharge and shuttle effect of lithium-sulfur batteries with V_2O_5-decorated carbon nanofiber interlayer. Small 13:1602539–1602545
13. Ma G, Wen Z, Wang Q, Chen S, Peng P, Jin J, Wu X (2015) Enhanced performance of lithium sulfur battery with self-assembly polypyrrole nanotube film as the functional interlayer. J Power Sources 273:511–516
14. Sun F, Wang J, Long D, Qiao W, Ling L, Lv C, Cai R (2013) A high-rate lithium–sulfur battery assisted by nitrogen-enriched mesoporous carbons decorated with ultrafine La_2O_3 nanoparticles. J Mater Chem A 1:13283–13289
15. Wan C, Wu W, Wu C, Xu J, Guan L (2014) A layered porous ZrO_2/RGO composite as sulfur host for lithium-sulfur batteries. RSC Adv 5:5102–5106
16. Zhang G, Wu HB, Song T, Paik U, Lou XW (2014) TiO_2 hollow spheres composed of highly crystalline nanocrystals exhibit superior lithium storage properties. Angew Chem Int Ed 53:12590–12593
17. Yu MP, Wang AL, Tian FY, Song HQ, Wang YS, Li C, Hongd J-D, Shi GQ (2015) Dual-protection of a graphene-sulfur composite by a compact graphene skin and an atomic layer deposited oxide coating for a lithium-sulfur battery. Nanoscale 7:5292–5298
18. Yin F, Liu X, Zhang Y, Zhao Y, Menbayeva A, Bakenov Z, Wang X (2017) Well-dispersed sulfur anchored on interconnected polypyrrole nanofiber network as high performance cathode for lithium-sulfur batteries. Solid State Sci 66:44–49
19. Vishnuvardhan TK, Kulkarni VR, Basavaraja C, Raghavendra SC (2006) Synthesis, characterization and A.C. conductivity of polypyrrole/Y_2O_3 composites. Bull Mater Sci 29:77–83
20. Fu Y, Manthiram A (2012) Orthorhombicbipyramidal sulfur coated with polypyrrole nanolayers as a cathode material for lithium–sulfur batteries. J Phys Chem C 116:8910–8915
21. Zhou G, Yin LC, Wang DW, Li L, Pei S, Gentle IR, Li F, Cheng HM (2013) Fibrous hybrid of graphene and sulfur nanocrystals for high-performance lithium-sulfur batteries. ACS Nano 7:5367–5375
22. Yin YX, Xin S, Guo YG, Wan LJ (2013) Lithium-sulfur batteries: electrochemistry, materials, and prospects. Angew Chem Int Ed 52:13186–13200
23. Xiao L, Cao Y, Xiao J, Schwenzer B, Engelhard MH, Saraf LV, Nie Z, Exarhos GJ, Liu J (2012) A soft approach to encapsulate sulfur: polyaniline nanotubes for lithium-sulfur batteries with long cycle life. Adv Mater 24:1176–1181
24. Mukkabla R, Meduri P, Deepa M, Shivaprasad SM, Ghosal P (2017) Sulfur enriched carbon nanotubols with a poly (3,4-ethylenedioxypyrrole) coating as cathodes for long-lasting Li-S batteries. J Power Sources 342:202–213
25. Li S, Ren G, Hoque MNF, Dong Z, Warzywoda J, Fan Z (2017) Carbonized cellulose paper as an effective interlayer in lithium-sulfur batteries. Appl Surf Sci 396:637–643
26. Ma G, Wen Z, Jin J, Wu M, Wu X, Zhang J (2014) Enhanced cycle performance of Li–S battery with a polypyrrole functional interlayer. J Power Sources 267:542–546
27. Yang K, Zhong L, Guan R, Xiao M, Han D, Wang S, Meng Y (2018) Carbon felt interlayer derived from rice paper and its synergistic encapsulation of polysulfides for lithium-sulfur batteries. Appl Surf Sci 441:914–922
28. Zhang Z, Wang G, Lai Y, Li J (2016) A freestanding hollow carbon nanofiber/reduced grapheneoxide interlayer for high-performance lithium–sulfur batteries. J Alloy Compd 663:501–506
29. Wang J, Yang Y, Kang F (2015) Porous carbon nanofiber paper as an effective interlayer for high-performance lithium-sulfur batteries. Electrochim Acta 168:271–276
30. Tang H, Yao SS, Xue SK, Liu MQ, Chen LL, Jing MX, Shen XQ, Li TB, Xiao KS, Qin SB (2018) In-situ synthesis of carbon@Ti_4O_7 non-woven fabric as a multi-functional interlayer for excellent lithium-sulfur battery. Electrochim Acta 263:158–167
31. Sun W, Ou X, Yue X, Yang Y, Wang Z, Rooney D, Sun K (2016) A simply effective double-coating cathode with MnO_2 nanosheets/graphene as functionalized interlayer for high performance lithium-sulfur batteries. Electrochim Acta 207:198–206
32. Li H, Wei Y, Zhang Y, Zhang C, Wang G, Zhao Y, Yin F, Bakenov Z (2016) In situ sol-gel synthesis of ultrafine ZnOnanocrystals anchored on graphene as anode material for lithium-ion batteries. Ceram Int 42:12371–12377